Supplementary Information for:

Imaging Ultra-weak UV Light Below 100 pW/cm² Using a 4H-SiC Photodetector with an Al_2O_3 Interfacial Layer

Xinyang Pei[1,#], Wenyan Wang[1,#,*], Kun Hu[2], Yuying Xi[2], Ting Ji[1], Guohui Li[2,*], Yanxia Cui[2,3]

[1]College of Physics, Taiyuan University of Technology, Taiyuan 030024, China;

[2]College of Electronic Information and Optical Engineering, Taiyuan University of Technology, Taiyuan 030024, China;

[3]Shanxi-Zheda Institute of Advanced Materials and Chemical Engineering, Taiyuan 030032, China;

[#]The two authors contribute equally to this work

Corresponding authors: wangwenyan@tyut.edu.cn; liguohui@tyut.edu.cn

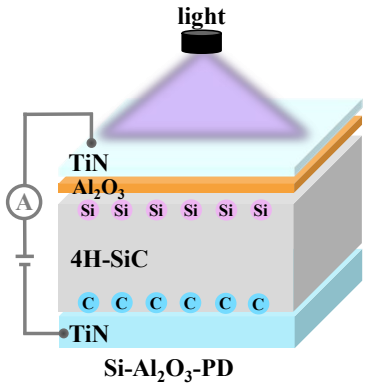

Fig. S1 Schematic diagram of the Si-Al_2O_3-PD reference device.

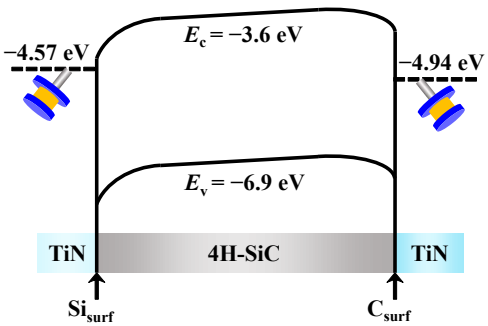

Fig. S2 Energy band diagram of the control 4H-SiC photodetector lacking Al_2O_3.

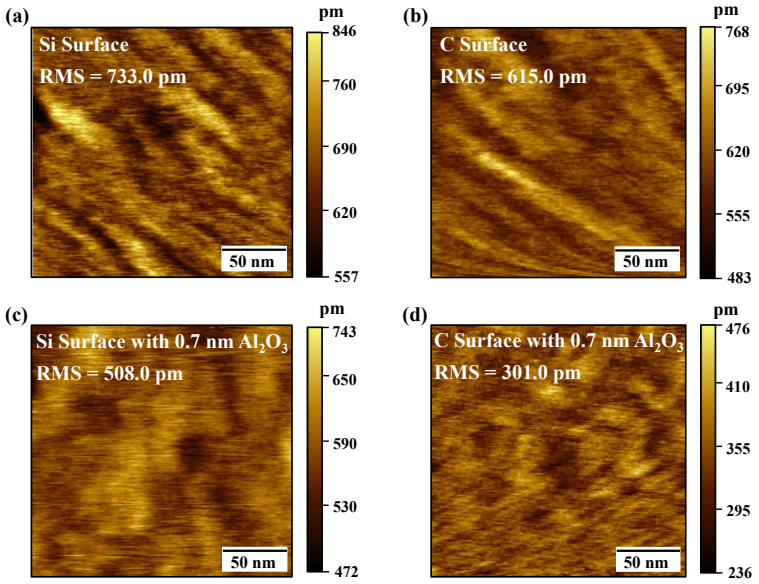

Fig. S3 (a-b) Surface morphology of Si surface and C surface of the 4H-SiC wafer, respectively. (c-d) Surface morphology of the 4H-SiC substrate with 0.7 nm Al_2O_3 on Si surface and C surface, respectively. All images were characterized by the AFM technique.

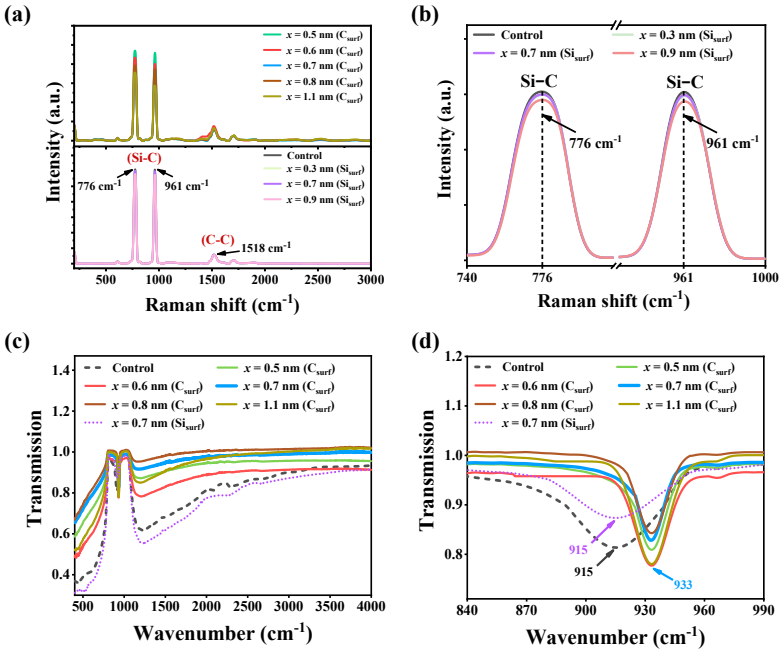

Fig. S4 (a) Raman spectra of 4H-SiC photodetectors with different thickness of ALD-Al_2O_3 on Si surface and C surface, respectively. (b) Expanded Raman spectra of 4H-SiC photodetectors with different thickness of ALD-Al_2O_3 on Si surface. (c) FT-IR spectra of pure 4H-SiC and the cases of C surfaces treated by different thickness of ALD-Al_2O_3. (d) Expanded plots of FT-IR spectra shown in (c).

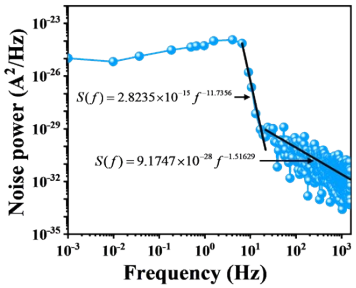

Fig. S5 Fitted noise current of the proposed C-Al_2O_3-PD at different frequencies.

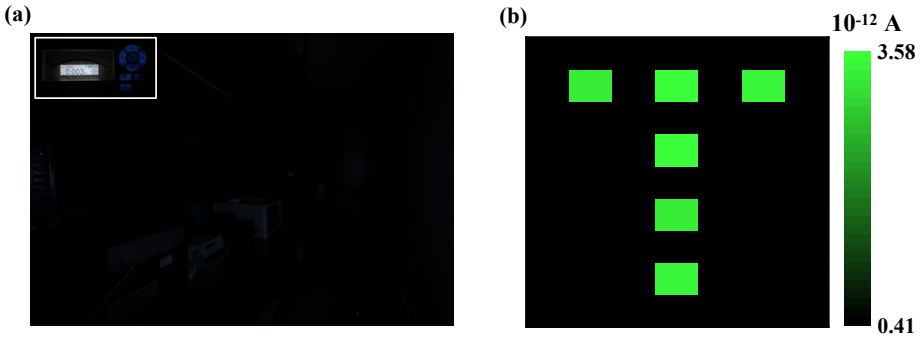

Fig. S6 (a) A real picture of the night vision environment with the light intensity of 3 nW. (b) Imaging result of the C-Al_2O_3-PD sensor in night vision environment.

Table S1. The photoelectric properties of typical SiC based photodetectors.

Structure	I_{dark} (A)	R (mA W^{-1})	D (Jnoes)	WDL (mW cm^2)	LDR (dB)	Rise/fall time (ms)	References
Cr/Cu/SiO_2/graphene/4H-SiC/Cr/Cu	5.9×10^{-10} (0 V)	80 (285 nm)	2.9×10^{12} (Shot noise)	—	—	4.5×10^{-3}/ 3.210^{-3}	1
Ag-4H-SiC nanohole-Ag	1×10^{-7} (5 V)	824 (375 nm)	6×10^{10} (Shot noise)	0.25−32.6	—	500/880	2
TiN/4H-SiC/TiN	7×10^{-14} (20 V)	32.7 (360 nm)	1.3×10^{13} (1/*f*)	9.68×10^{-8} −15.7	164	0.52	3
Cr/Au/SiO_2/graphene/n^-/n^+ 4H-SiC/ Cr/Au	5.8×10^{-8} (0 V)	0.75 V/W (300 nm)	2.7×10^{13} (Shot noise)	6×10^{-6} -1.2×10^{-5}	—	7.4×10^{-5}/ 5.81×10^{-4}	4
Au NPs/Ti/Au/ n^-/n^+ 4H-SiC	5×10^{-15} (5 V)	63 (270 nm)	4×10^{13} (Shot noise)	—	—	1.9×10^{-6}/2.2×10^{-6}	5
Ni/Ti/Al/Au/SiO_2/ n-p-n 4H-SiC/ Ni/Ti/Al/Au	1×10^{-12} (5 V)	130 (275 nm)	7.27×10^{13} (1/*f*)	1×10^{-4}–10	44	1.179/0.668	6
TiN/Au/PEDOT:PPS/SiC/ In	8.3×10^{-6} (1.1 V)	2150 (254 nm)	1.9×10^{13} (Shot noise)	5×10^{-3}–0.6	—	58.6/41.5	7
Ti/Au/$ZnGa_2O_3$/4H-SiC/In	$\sim10^{-10}$ (0 V)	115 (254 nm)	—	0.04–1.64	—	18.36/16.15	8
Au/Au NPs/quasifreestanding graphene/Vicinal SiC	—	1.65 (365 nm)	2.82×10^{8} (Shot noise)	—	—	3.5×10^{3}/ 4.3×10^{3}	9
Ni/Ti/Al/Au/SiO^2/p^-/p^+/n^+ 4H-SiC	6×10^{-13} (−10 V)	104 (13.5 nm)	3.4×10^{12} (1/*f*)	—	—	—	10
Ti/Au/graphene/4H-SiC	5×10^{-14} (10 V)	134 (250 nm)	1.2×10^{11} (1/*f*)	—	—	0.01/0.033	11
Ag/4H-SiC nanowire arrays/Ag	9.1×10^{-8} (3 V)	220 (275 nm)	8.45×10^{7} (Shot noise)	1.4–6.4	—	47.3/49.3	12
ITO/SiO_2/p-i-n 4H-SiC nanocone/Ni	1×10^{-12} (−0.5 V)	41.9 (360 nm)	—	$0.1–1\times10^{4}$	—	1.7/1.8	13

$W/W_xSi_yO_{1-x-y}$/passivation layer/4H-SiC	3×10^{-13} (−15 V)	230 (275 nm)	—	—	—	7.6/4.7	14
Pd/Au/epitaxial graphene/4H-SiC	—	2457 (405 nm)	1.72×10^{7} (Shot noise)	7.96–199	—	1.7×10^{4}/ 1.6×10^{4}	15
Ti/Au/SnS_2/4H-SiC	$\sim10^{-10}$ A/μm^2 (5 V)	2.42×10^{4} (325 nm)	7.3×10^{13} (Shot noise)	0.1–10	—	17	16
Ti/SiO_2/graphene/4H-SiC/Ti	$<3\times10^{-3}$ (3 V)	254.1 (325 nm)	2.16×10^{10} (Shot noise)	—	—	2350/1110/ 1500/22020	17
Ti/Ag/Si_3N_4/Pd/4H-SiC/Ti/Ag	1×10^{-12} (−2 V)	113 (248 nm)	—	—	—	—	18
NiAl/4H-SiC	6.2×10^{-13} (−0.5 V)	2.75×10^{7} (280 nm)	—	—	147	—	19
β-Ga_2O_3/p-SiC/4H-SiC	6.2×10^{-12} (0 V)	10.35 (254 nm)	8.8×10^{9} (Shot noise)	7.9×10^{-3} – 91×10^{-3}	64.38	11/19	20
Ni/Ni_2Si/n-4H-SiC/Ni	1.2×10^{-10} (15 V)	120 (300 nm)	—	—	—	1.9×10^{-4}	21
p-type graphene/ZnS QDs/4H-SiC	1.7×10^{-10} (0 V)	0.29 (250 nm)	1.41×10^{10} (Shot noise)	0.155–0.184		0.28/0.75	22
n^+-3C-SiC/SiO_2/n-3C-SiC/p-Si/Al	7.6×10^{-6} (2 V)	3.2 (375 nm)	—	0.6−7.2	—	320/360	23
Graphene/β-Ga_2O_3/4H-SiC/Au	5.1×10^{-10} (0V)	180 (254 nm, −5 V)	—	1×10^{-2}–7×10^{-2}		650/7800/173/15220	24
TiN/4H-SiC/Al_2O_3/TiN	1.8×10^{-14} (20 V)	4.89 (360 nm)	1.3×10^{13} (Shot noise) 1.49×10^{10} (1/*f*)	3.18×10^{-8} −10.2	172	0.3/0.29	**This work**

References

1 A. K. Jehad, M. Fidan, Ö. Ünverdi and C. Çelebi, *Sensors Actuators A: Physical*, 2023, **355**, 114309.

2 K. Wang, H. Wang, C. Chen, W. Li, L. Wang, F. Hu, F. Gao, W. Yang, Z. Wang and S. Chen, *ACS Applied Materials & Interfaces*, 2023, **15**, 23457−23469.

3 M. Li, L. Geng, Y. Xi, K. Hu, L. Shi, W. Wang, Y. Tian, T. Ji, K. Mao and B. Xu, *Journal of Physics D: Applied Physics*, 2023, **56**, 375105.

4 A. K. Jehad, O. Unverdi and C. Celebi, *Journal of Alloys anf Compounds*, 2023, **969**, 172288.

5 M. Yuan, M. Zhang, Z. Fu, S. Han, Y. Zhang, S. Wu, R. Hong, X. Chen, J. Cai and D. Lin, *ACS Applied Nano Materials*, 2023, **6**, 9376-9384.

6 Y. Wang, W. Li, D. Zhou, W. Xu, F. Ren, D. Chen, R. Zhang, Y. Zheng and H. Lu, *IEEE Transactions on Electron Devices*, 2022, **70**, 159-166.

7 S. Li, L. Yang, Z. Liu, M. Zhang, Y. Guo and W. Tang, *Applied Physics Letters*, 2023, **122**.

8 D. Han, Y. Yang, L. Meng, S. Hu, K. Liu, H. Lin, N. Liu, W. Zhang and J. Ye, *Applied Physics Letters*, 2023, **123**.

9 I. Khadka, N. Alluri, M. Alsardia, N. J. Raj, A. Prasanna, B. U. Haq, S. Kim and S.-H. Kim, *Applied Surface Science*, 2023, **610**, 155275.

10 Z. Wang, D. Zhou, W. Xu, Y. Wang, F. Ren, D. Chen, R. Zhang, Y. Zheng and H. Lu, *IEEE Electron Device Letters*, 2022, **43**, 906-909.

11 H. He, N. Shetty, S. Kubatkin, P. Stadler, T. Löfwander, M. Fogelström, J. C. Miranda-Valenzuela, R. Yakimova, T. Bauch and S. Lara-Avila, *Applied Physics Letters*, 2022, **120**, 191101.

12 L. Li, S. Yuan, K. Amina, P. Zhai, Y. Su, R. Lou, X. Hao, H. Shan, T. Xue and H. Liu, *Sensors Actuators A: Physical*, 2022, **346**, 113878.

13 S. Guo, X. Zhao, Y. He, Y. Cai, M. Yang, X. Guo, X. Fu and L. Zhang, *IEEE Transactions on Electron Devices*, 2021, **68**, 6208-6215.

14 F. Du, Q. Song, X. Tang, Z. Zhang, H. Yuan, C. Han, C. Zhang, Y. Zhang and Y. Zhang, *IEEE Transactions on Electron Devices*, 2021, **68**, 5662-5665.

15 S. Rathore, D. K. Patel, M. K. Thakur, G. Haider, M. Kalbac, M. Kruskopf, C.-I. Liu, A. F. Rigosi, R. E. Elmquist and C.-T. Liang, *Carbon*, 2021, **184**, 72-81.

16 Q. Yue, W. Gao, P. Wen, Q. Chen, M. Yang, Z. Zheng, D. Luo, N. Huo, F. Zhang and J. Li, *Journal of Materials Chemistry C*, 2021, **9**, 15662-15670.

17 Y. Li, P. Chen, X. Chen, R. Xu, M. Liu, J. Zhou, C. Ge, H. Peng, X. Mao and J. Feng, *Advanced optical materials*, 2020, **8**, 2000559.

18 S. P. Karanth, M. A. Sumesh, V. Shobha, J. Sirisha, D. Yadav M, S. B. Vijay and K. V. Sriram, *IEEE Transactions on Electron Devices*, 2020, **67**, 3242-3249.

19 L. Di Benedetto, G. D. Licciardo, T. Erlbacher, A. J. Bauer and A. Rubino, *IEEE Transactions on Electron Devices*, 2019, **67**, 154-159.

20 J. Yu, L. Dong, B. Peng, L. Yuan, Y. Huang, L. Zhang, Y. Zhang and R. Jia, *Journal of Alloys and Compounds*, 2020, **821**, 153532.

21 A. Sciuto, A. Meli, L. Calcagno, S. Di Franco, M. Mazzillo, G. Franzo, S. Albergo, A. Tricomi, D. Longo and G. Giudice, *IEEE Sensors Journal*, 2019, **19**, 2931-2936.

22 H. Kan, W. Zheng, R. Lin, M. Li, C. Fu, H. Sun, M. Dong, C. Xu, J. Luo and Y. Fu, *ACS applied materials & interfaces*, 2019, **11**, 8412-8418.

23 A. R. M. Foisal, T. Dinh, P. Tanner, H.-P. Phan, T.-K. Nguyen, E. W. Streed and D. V. Dao, *IEEE Electron Device Letters*, 2018, **39**, 1219-1222.

24 Y. Qu, Z. Wu, M. Ai, D. Guo, Y. An, H. Yang, L. Li and W. Tang, *Journal of Alloys and Compounds*, 2016, **680**, 247-251.